Values of ϵ_P are included in Table I and are seen to be smaller than the experimental activation energies by a factor of almost two. However, as Price was careful to point out, there are many uncertainties in the theoretical development of the Mott model.

Finally, we draw attention to the fact that our experimental activation energies are derived empirically from the specific resistivity, which depends upon both the density of carriers and the mobility, so that, if the mobility is a strong function of temperature, the activation energy relevant to the density of carriers is different. If, for example, the mobility were to vary as $1/T$, as suggested by Conwell,[9] then the activation energies for the density of carriers alone would be about 15% larger than the values we have quoted.

ACKNOWLEDGMENTS

We are grateful to the Bell Telephone Laboratories for preparing the ingots, to Philco Corporation for the loan of a vibrating reed electrometer and for cutting out some of our specimens, and to Dr. E. Burstein and Dr. A. Filler for the spectroscopic determination of the oxygen content of the specimens. We have benefited greatly from discussions with Dr. T. H. Geballe, Dr. W. Kohn, and Dr. G. Swartz.

PHYSICAL REVIEW VOLUME 118, NUMBER 2 APRIL 15, 1960

Pulsed Nuclear Resonance Spectroscopy*

M. Emshwiller,† E. L. Hahn, and D. Kaplan‡
Department of Physics, University of California, Berkeley, California

(Received November 2, 1959)

A technique for the detection of weak nuclear resonance interactions in solids is carried out by a pulsed method which obtains nuclear double resonance. The resonance of the unknown species to be detected does not require a Boltzmann population difference in spin orientation, but must have a sufficient dipole-dipole interaction with a second spin species. At resonance, a single 180° pulse reorients the unknown spins at the time of the 180° pulse in the 90°–180° pulse sequence necessary to obtain the observed spin-echo signal of the second species. A reduction of the spin-echo signal signifies double resonance due to changes in local dipolar fields, coupled to the observed spins, which scrambles their precessional phases. Nuclear quadrupole coupling interactions of K, Cs, and Rb isotopes are measured in the chlorates of these ions, where the Cl^{35} nucleus provides the observed nuclear quadrupole echo. An analysis is presented for the case of low concentration of unknown spin species. Double quantum transitions and special properties of nuclear quadrupole spectra are observed.

A SENSITIVE method for the detection of weak nuclear resonance interactions is successful in solids where strong spin-echo signals can be observed. This is carried out by observing the change in spin-echo dipolar relaxation of a spin group A, due to the effect of the pulsed resonance of a nuclear neighbor (spin group B) obtained in the same crystal.[1] The particular experiments reported here deal with pure quadrupole resonance,[2] but the principles involved apply to any spin resonance system satisfying certain requirements. At all times, the relaxation of the A spins is observed in terms of the attenuation of a two-pulse 90°–180° spin-echo amplitude. The B spins are subjected to double resonance by the action of a single pulse. They may also undergo a continuous rf (radio-frequency) excitation,[3] which is less effective and hence has not been used for the purposes of spectroscopy reported here. The A spins are particularly sensitive to any disturbance of the Larmor frequency and phase relationships which are necessary for spin-echo formation. For a given time spacing τ between 90° and 180° pulses, the echo amplitude at time 2τ for the A spins will correspond to a certain degree of phase memory. If the A-B dipole-dipole coupling is modulated or suddenly changed by double resonance, phase relations are upset and the echo amplitude is modified. In the case of pulsed double resonance in solids, the echo is reduced in amplitude.

I. PULSED DOUBLE RESONANCE IN LIQUIDS

The effect of pulsed double resonance is clearly indicated by the study of proton (A-spin) echoes coupled to phosphorus nuclei (B spins) in an aqueous solution of phosphorous acid, $HPO(OH)_2$. The indirect spin-spin interaction occurs between H and P nuclei in the HPO group, described by $J\mathbf{I}_H\cdot\mathbf{I}_P$ in frequency units, where $\mathbf{I}$ is the spin operator, and $J/2\pi=708$ cps (cycles per

---

[9] (see previous article)

* Supported in part by the Office of Naval Research and the National Security Agency.

† Present address: Bell Telephone Laboratories, Whippany, New Jersey.

‡ Present address: Lockheed Missile Systems Division, Palo Alto, California.

[1] D. Kaplan and E. L. Hahn, Bull. Am. Phys. Soc. 2, 384 (1957); J. phys. radium 19, 821 (1958).

[2] M. Bloom, E. L. Hahn, and B. Herzog, Phys. Rev. 97, 1699 (1955).

[3] B. Herzog and E. L. Hahn, Phys. Rev. 103, 148 (1956).

second) is known.[4] The H concentration involved in the coupling is about $\frac{1}{8}$ of the total proton concentration in the sample used. A 90°–180° double-pulse sequence is applied to obtain the proton echo, and a third pulse is applied at the P resonance at a time t' with respect to the first 90° proton pulse. Consider only the macroscopic magnetic moment M_0 due to those protons coupled to the phosphorus, and let them have an off-resonance angular frequency $\Delta\omega$ with respect to a frame of reference rotating at a Larmor frequency ω_H in the absence of J coupling. In the time interval from 0 to t', one-half of the protons precess at a frequency $\Delta\omega+J/2$ in this frame, and the other half precess at a frequency $\Delta\omega-J/2$ because of the J coupling due to two possible orientations of P nuclei with spin $I_P=\frac{1}{2}$. Let the P nuclei be excited into a superposition of these two states by action of a θ pulse at t', where $\theta=\gamma_P H_1 t_w$, H_1 is the rf field intensity of the rotating component, γ_P is the phosphorus gyromagnetic ratio, and t_w is the pulse width. A simple solution to the time-dependent Schrödinger equation leads to the result[5] that the fraction of P nuclei which undergo the quantum transition $(\pm\frac{1}{2}\rightarrow\mp\frac{1}{2})$ is $\beta=\sin^2(\theta/2)$, and the fraction which remains unchanged in orientation $(\pm\frac{1}{2}\rightarrow\pm\frac{1}{2})$ is $\alpha=\cos^2(\theta/2)$. If we let $t'=\tau$ and neglect relaxation, the proton echo calculation[6] yields, for $t\geqq\tau$,

$$\begin{aligned}V_A(t)=\tfrac{1}{2}M_0(&\exp[-i(\Delta\omega+\tfrac{1}{2}J)\tau]\\&\times\{\alpha\exp[i(\Delta\omega+\tfrac{1}{2}J)(t-\tau)]\\&+\beta\exp[i(\Delta\omega-\tfrac{1}{2}J)(t-\tau)]\}\\&+\exp[-i(\Delta\omega-\tfrac{1}{2}J)\tau]\\&\times\{\alpha\exp[i(\Delta\omega-\tfrac{1}{2}J)(t-\tau)]\\&+\beta\exp[i(\Delta\omega+\tfrac{1}{2}J)(t-\tau)]\}). \qquad (1)\end{aligned}$$

At $t=2\tau$, the proton echo maximum is

$$V_A(2\tau)=M_0(\alpha+\beta\cos J\tau), \qquad (2)$$

which is a convenient formula to apply when τ is varied. If $t'\neq\tau$, then

$$V_A(2\tau)=M_0[\alpha+\beta\cos J(\tau-|\tau-t'|)] \qquad (3)$$

is convenient when t' is varied in the experiment. The measurement indicated by Fig. 1 was carried out for a $\theta=180°$ pulse ($\alpha=0$, $\beta=1$) by superposition of photographs of the proton echo for a range of t' values. The beat modulation due to the coupled protons is proportional to the function $\cos Jt'$ for $t'\leqq\tau$, which undergoes a phase shift of $J\tau$ at $t'=\tau$.

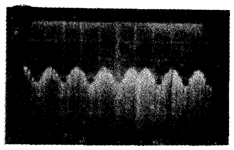

FIG. 1. Modulation of proton echo envelope due to double resonance of P nuclei in HPO(OH)$_2$ as a function of time t' [see Eq. (3)]. The oscillogram pattern extends over a total time of 10 milliseconds. The phase shift occurs at a time $\tau=6.2$ milliseconds. Zero echo amplitude baseline is below the oscilloscope face.

By extending the above calculation to a system of N neighbors of type B with $I=\frac{1}{2}$, the echo amplitude of the A spins is given by

$$V_A(2\tau)=M_0\prod_{j=1}^{N}(\alpha+\beta\cos J_j\tau). \qquad (4)$$

For large N, $\alpha=0$, and $\beta=1$, the average echo amplitude is given roughly by

$$\langle V_A(2\tau)\rangle_{\text{Av}}=M_0\exp(-\tau^2J_{\text{Av}}^2/2),$$

where J_{Av}^2 is the mean-square average of J_j. For a configuration of B spins with $I_B>\frac{1}{2}$, it is convenient to use the Majorana-Bloch-Rabi formula[7] for evaluating transition probabilities which play the role of α and β in the above case.

The effects of the tensor dipole-dipole interaction in solids cannot be given the straightforward treatment, which leads to the result given by Eq. (4). We see, however, that the observed echo, which is influenced by the double resonance, is made up of a superposition of component echoes, where each echo has a given phase determined by one of a distribution of local fields caused by neighboring B spins. For a general spatial distribution of many neighbors, the value of $V_A(2\tau)$ is always smaller than its value for $\beta=0$ and $\alpha=1$ (when the double resonance is not obtained).

In former spin-echo modulation experiments[6] in liquids, the double resonance effect was essentially taking place. In those experiments, two inequivalent proton groups, having different chemical shifts defined as $\delta_1-\delta_2=\delta$, also displayed a J interaction. For the condition $\delta\gg J$, the above calculation predicts the behavior of the echo modulation, if one group is first looked upon as the A spins and the other group as the B spins. Finally, the signal from this calculation must be added to the signal obtained when the roles of these groups are reversed, and the observed spin-echo modulation is obtained.

II. PULSED DOUBLE RESONANCE IN SOLIDS

In our spectroscopy experiments, single crystals or the powder form of the alkali chlorates have been studied, where the Cl^{35} echo was observed as the A group, and the B spins included Na^{23}, K^{39}, K^{41}, Cs^{133}, Rb^{85}, and Rb^{87}. A pulsed pure quadrupole resonance search was made for the alkali ion by varying the carrier frequency ν_B of a 180° pulse, applied at time τ, when a 180° pulse was also applied to the Cl^{35} spins. The Cl^{35} quadrupole resonance in the ClO$_3$ group occurs[8] in the

---

[4] H. S. Gutowsky, D. W. McCall, and C. P. Slichter, J. Chem. Phys. **21**, 279 (1953).

[5] I. I. Rabi, Phys. Rev. **51**, 652 (1937).

[6] E. L. Hahn and D. E. Maxwell, Phys. Rev. **88**, 1070 (1952); E. L. Hahn, Phys. Rev. **80**, 580 (1950).

[7] F. Bloch and I. I. Rabi, Revs. Modern Phys. **17**, 237 (1945).

[8] T. P. Das and E. L. Hahn, *Solid-State Physics*, edited by F. Seitz and D. Turnbull (Academic Press, New York, 1958), Suppl. 1, p. 102.

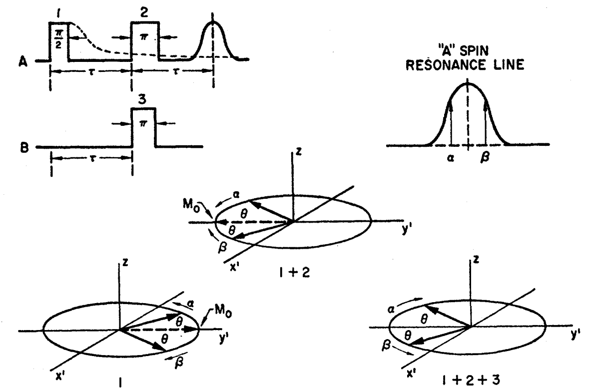

FIG. 2. Double resonance pulse effect of spin echo attenuation.

range of 20 to 35 Mc/sec, whereas ν_B occurs below one megacycle/second.

A simple description of the double resonance effect in solids can be given in terms of the spin-echo vector model. First, all effects due to T_2 (mutual spin-spin flipping) and T_1 (spin-lattice) relaxation times are neglected. Let static local magnetic fields at A spin sites originate from the z components of magnetic moments μ_B of unlike neighboring B spins. Assume all spins are quantized in the direction of a strong external field. To a first approximation, this can be realized for A–B spins occurring in isolated pairs, where each pair has a random distance of separation r_{AB} about a mean, so that there is a distribution in local field $h_{AB}\sim\mu_B/r_{AB}^3$ at the A sites, giving an inhomogeneously broadened line. Figure 2 indicates a 90°–180° pulse sequence (1+2) acting on the A spins, which causes the normal rephasing of particular moment vectors α and β contributing to the spin-echo amplitude $E_{AB}(2\tau)=1$ at $t=2\tau$. If, however, a 180° pulse is applied to the B spins (pulse 3) at time τ, all local fields h_{AB} at the A-spin sites reverse sign, as viewed in the frame of reference rotating at Larmor frequency ν_A of the A spins. Consequently, the reversal of phase of the A spins made possible by the 180° pulse (pulse 2) is prevented by pulse 3. The spin echo therefore disappears, and the free-induction signal remains after pulse 1 (indicated by the dotted curve in Fig. 2). If we assume a Gaussian distribution,

$$P(h_{AB})=(2\pi\langle h_{AB}^2\rangle_{\mathrm{Av}})^{-\frac{1}{2}}\exp[-(h_{AB}^2/2\langle h_{AB}^2\rangle_{\mathrm{Av}})],$$

in the local field, the free-induction signal amplitude which remains at $t=2\tau$ is given by

$$T_{AB}(2\tau)=\int_{-\infty}^{\infty}P(h_{AB})\cos(\gamma_A h_{AB}\cdot 2\tau)dh_{AB}$$
$$=\exp(-2\langle\delta_{AB}^2\rangle_{\mathrm{Av}}\tau^2),\quad(5)$$

where $\langle\delta_{AB}^2\rangle_{\mathrm{Av}}=(\gamma_A^2\langle h_{AB}^2\rangle_{\mathrm{Av}})$ is the second moment of the A resonance line. This model can be extended to include the static dipolar coupling involving A–A, A–B, and A–B' types of interaction, where B' is a third spin species. Now the application of pulses 1 and 2 alone implies a virtual double resonance acting on the A spins, because the local field component $h_{AA}\sim\mu_A/r_{AA}^3$ changes sign. The echo signal amplitude at $t=2\tau$ is then given by

$$V(2\tau)=E_{ABB'}(2\tau)T_{AA}(2\tau),\quad(6)$$

where $E_{ABB'}(2\tau)=1$ is the normalized echo amplitude if the A–A interaction is absent. If A spins are present only, $T_{AA}(2\tau)=\exp[-\langle\delta_A^2\rangle_{\mathrm{Av}}(2\tau)^2/2]$ would be the observed free precession signal following a single 90° pulse, where $\langle\delta_A^2\rangle_{\mathrm{Av}}=\gamma_A^2\langle h_{AA}^2\rangle_{\mathrm{Av}}$. Later, when spin-spin relaxation is considered, Eq. (6) will have $E_{ABB'}(2\tau)<1$, and the A echo also is severely limited in amplitude by $T_{AA}(2\tau)$, which still behaves very much the same as above. Obviously, in a sample containing only a single species of A spins, it is impossible to obtain a 90°–180° echo. This can be rigorously shown, even in the presence of spin-spin relaxation. However, an echo somewhat reduced in amplitude would occur with application of a $90°-\theta$ pulse sequence, where $\theta\neq n\pi$ and n is an integer.

If the pulses 1+2+3 are applied, where 3 excites the B system, a later analysis will show that the A echo is given by

$$V_d(2\tau)=E_{AB'}(2\tau)T_{AB}(2\tau)T_{AA}(2\tau).\quad(7)$$

The echo given by $V(2\tau)$ is reduced by double resonance to an amplitude $V_d(2\tau)$ because of the attenuation mainly due to $T_{AB}(2\tau)=\exp(-2\langle\delta_{AB}^2\rangle_{\mathrm{Av}}\tau^2)$. The resonance of the B system is measured as a function of ν_B when the difference between (6) and (7),

$$\Delta V=V(2\tau)-V_d(2\tau),\quad(8)$$

is a maximum.

III. EFFECT OF RELAXATION ON THE DOUBLE RESONANCE

A rigorous description of spin echoes in solids which includes spin-spin relaxation is an unsolved problem, while the rigorous treatment of the effect of double resonance would be even more difficult. Lowe and Norberg[9] have treated in a rigorous fashion the case of free precession following a sharp 90° pulse in pure magnetic resonance. Instead an expression is formulated here for the echo in terms of the properties of the free precession signal following a 90° pulse by applying methods of correlation function theory.

Consider a collection of A spins throughout the sample which precess in phase after a 90° pulse at an initial angular frequency $\delta(0)$ at $t=0$. At some later time, this frequency will assume another value $\delta(t)$ because of spin-spin interactions caused by coupling with all types of neighbors. Here T_1 is assumed to be infinite. In this case, the relevant dipolar Hamiltonian for an A–B system is

$$\mathcal{H}_{dd}=\sum_{k>j}(C_{jk}\mathbf{I}_j\cdot\mathbf{I}_k+D_{jk}I_{zj}I_{zk})+\sum_{k'>j'}(C_{j'k'}\mathbf{I}_{j'}\cdot\mathbf{I}_{k'}$$
$$+D_{j'k'}I_{zj'}I_{zk'})+\sum_{j,k'}E_{jk'}I_{zj}I_{zk'},\quad(9)$$

---

[9] I. I. Lowe and R. E. Norberg, Phys. Rev. **107**, 46 (1957).

where

$$C_{jk}=(\gamma^2\hbar^2 r_{jk}^{-3}/2)(3\cos^2\theta_{jk}-1), \tag{10}$$

$$D_{jk}=-\tfrac{3}{2}\gamma^2\hbar^2 r_{jk}^{-3}(3\cos^2\theta_{jk}-1), \tag{11}$$

and

$$E_{jk'}=(1-3\cos^2\theta_{jk'})\gamma\gamma'\hbar^2 r_{jk'}^{-3}. \tag{12}$$

Radius vector $\mathbf{r}_{jk}$ is the line joining the two spins, which makes an angle θ_{jk} with respect to the axis of quantization. The jk and $j'k'$ terms refer to the A and B spins, respectively, and the jk' terms refer to coupling between A and B spins. The extension of this Hamiltonian to include a second B' foreign species is obvious. The fluctuations in $\delta(t)$ occur because the terms involving C_{jk} and $C_{j'k'}$ do not allow the Hamiltonian $\mathcal{H}_{dd}$ to commute with the operators $I_{zj}I_{zk}$, $I_{zj'}I_{zk'}$ and $I_{zj}I_{zk'}$.

The transverse magnetic moment of a group of A spins characterized by $\delta(0)$ at $t=0$ can be written as

$$S(t)=\exp\left[i\int_0^t \delta(t')dt'\right], \tag{13}$$

in the frame of reference rotating at frequency ν_A. The average value of $S(t)$ over the spin ensemble, written as $\langle S(t)\rangle=T(t)$, expresses the measured free-precession signal. Let

$$\delta(t')=\delta_A(t')+\delta_B(t')+\delta_{B'}(t'), \tag{14}$$

which assumes that the Larmor frequency $\delta(t')$ in the moving frame is a superposition of local fields caused by neighboring A, B, and B' spins. At $t=\tau$, the 180° pulse acting only upon the A spins imposes the transformation in the phase [excluding the sign reversal of $\delta_A(\tau)$] of Eq. (13) as follows:

$$\exp\left[+i\int_0^\tau \delta(t')dt'\right]\to\exp\left[-i\int_0^\tau \delta(t')dt'\right]. \tag{15}$$

For $t\geqq\tau$, the average transverse magnetic moment, defined by the average of (13), is written as $V(t)$ to define the observed echo, rather than $T(t)$, namely,

$$V(t)=\left\{\exp\left[-i\int_0^\tau \delta(t')dt'\right]\exp\left[+i\int_\tau^{\tau+t} \times[-\delta_A(t')+\delta_B(t')+\delta_{B'}(t')dt]\right]\right\}_{\text{Av}}. \tag{16}$$

Note that a minus sign prefixes the term $\delta_A(t')$ because the local field due to A spins is reversed by the 180° pulse. The echo at $t=2\tau$ can be written as

$$V(2\tau)=E_{AB}(2\tau)E_{AB'}(2\tau)T_{AA}(2\tau), \tag{17}$$

where

$$E_{AB}(2\tau)=\left\{\exp i\left[\int_\tau^{2\tau} \delta_B(t')dt'-\int_0^\tau \delta_B(t')dt'\right]\right\}_{\text{Av}}, \tag{18}$$

$$E_{AB'}(2\tau)=\left\{\exp i\left[\int_\tau^{2\tau} \delta_{B'}(t')dt'-\int_0^\tau \delta_{B'}(t')dt'\right]\right\}_{\text{Av}}, \tag{19}$$

and

$$T_{AA}(2\tau)=\left\{\exp i\int_0^{2\tau} \delta_A(t')dt'\right\}_{\text{Av}}. \tag{20}$$

Equations (18), (19), and (20) are written as averages, if we assume that these terms are uncorrelated. For no double resonance in this case, the echo $V(2\tau)$ appears to be a product of three virtual signals: the two signals $E_{AB}(2\tau)$ and $E_{AB'}(2\tau)$ appear to be individual echo terms due to the presence of B and B' spins only, with the A–A interaction absent; and the third signal $T_{AA}(2\tau)$ is the free-precession A signal term which occurs for the A–A interaction present and the A–B, A–B' interactions absent. Here, the statement "interactions absent" means only the expressions given formally above. For example, the frequency $\delta_A(t')$, which expresses the A–A interaction, is actually modified by the local fields of B and B' through the effect of the C, D, and E terms in (9).

If we obtain the B-spin double resonance with a 180° pulse and formulate ΔV according to (8), we obtain

$$\Delta V=[E_{AB}(2\tau)-T_{AB}(2\tau)]E_{AB'}(2\tau)T_{AA}(2\tau), \tag{21}$$

where $T_{AB}(2\tau)=\langle\exp[i\int_0^{2\tau}\delta_{AB}(t')dt']\rangle$. Consider the case where we wish to detect a very low concentration of B spins compared to a much higher concentration of B' and A spins. The line width of the A resonance is therefore determined mainly by A and B'. Here, the echo measurement is made at a time 2τ such that the exponential terms $E_{AB}(2\tau)$ and $T_{AB}(2\tau)$ are not much smaller than unity. Upon expanding these functions to first order, noting that they must be even functions, the difference

$$E_{AB}(2\tau)-T_{AB}(2\tau) =\frac{1}{2}\left\{\left[\int_0^{2\tau}\delta_{AB}(t')dt'\right]^2_{\text{Av}} -\left[\int_0^\tau \delta_{AB}(t')dt'\int_\tau^{2\tau}\delta_{AB}(t')dt'\right]^2_{\text{Av}}\right\} \tag{22}$$

results. It can be shown[10] easily that the second average above can be written as

$$\left[\int_0^{2\tau}\delta_{AB}(t')dt\right]^2_{\text{Av}}-4\left[\int_0^\tau \delta_{AB}(t')dt'\right]^2_{\text{Av}}. \tag{23}$$

Therefore,

$$\Delta V\approx 2\left[\int_0^\tau \delta_{AB}(t')dt'\right]^2_{\text{Av}} E_{AB'}(2\tau)T_{AA}(2\tau). \tag{24}$$

---

[10] A. Abragam, Cours sur les phénomènes liés à la résonance magnétique (Notes), Saclay, France (unpublished).

From correlation function theory,[11]

$$\left[\int_0^\tau \delta_{AB}(t')dt'\right]_{\text{Av}}^2 = 2\int_0^\tau (\tau-\tau')\langle\delta_{AB}(\tau)\delta_{AB}(\tau+\tau')\rangle d\tau', \quad (25)$$

where $\langle\delta_{AB}(\tau)\delta_{AB}(\tau+\tau')\rangle$ is the autocorrelation function for the frequency. For τ sufficiently short, so that the B spins retain to an appreciable extent their orientations at $t=0$, Eqs. (24) and (25) can be combined to give

$$\langle\delta_{AB}(\tau)\delta_{AB}(\tau+\tau')\rangle\approx\langle\delta_{AB}^2\rangle_{\text{Av}};$$

and

$$\Delta V=2\langle\delta_{AB}^2\rangle_{\text{Av}}\tau^2 E_{AB'}(2\tau)T_{AA}(2\tau), \quad (26)$$

where $\langle\delta_{AB}^2\rangle_{\text{Av}}$ is the second-moment contribution to the line shape of the A resonance. This orientation memory is enhanced by the presence of A and B' dipolar fields, which tend to decouple the B spins from one another. In a quadrupole system, it is a good approximation in one extreme case to assume that $E_{AB'}(2\tau)=1$, and $T_{AA}(2\tau)=\exp[-(2\langle\delta_A^2\rangle_{\text{Av}}\tau^2)]$, when a small dc magnetic field is applied to the sample. New Zeeman levels are created for each species of the quadrupole system. The spin-spin interaction involving exchange [the C terms in (9)] is then markedly reduced because new resonance lines are produced.[8] The signal ΔV is a maximum for $\tau^2=\frac{1}{2}\langle\delta_A^2\rangle_{\text{Av}}$, so that

$$\Delta V_{\max}=\frac{1}{e}M_{0A}\omega_A G\langle\delta_{AB}^2\rangle_{\text{Av}}/\langle\delta_A^2\rangle_{\text{Av}}, \quad (27)$$

where we now include M_{0A}, the magnetic moment of the A spins; ω_A, the Larmor frequency of precession; and G, a geometric factor.

It is extremely difficult to treat the general case where exchange terms are important in determining the magnitude of $\Delta V_{\max}$. Some idea of the complexity is given in Appendix A, concerning a description of the echo itself in terms of higher moments of the line width. In the absence of double resonance, evidence that the echo attenuates mainly because of the term $T_{AA}(2\tau)$ is borne out by the fact that the stimulated echo,[6] obtained after the application of a third pulse, has a much larger envelope lifetime than that of the echo measured at 2τ, by as much as a factor of ten. Exclusive of the effect of T_1, the stimulated echo lifetimes serve as a measure of local field fluctuations. These fluctuations prove not to be important compared to the attenuation effect of the term $T_{AA}(2\tau)$.

IV. SENSITIVITY OF THE METHOD

There would be no advantage to the pulse-spectroscopy method for the B spins if the same sensitivity were obtained by steady-state magnetic resonance absorption in a large magnetic field, or by a direct pure quadrupole resonance measurement of the B spins. There is an advantage, however, in certain cases. Assuming the same geometrical factor G and equivalent sensitivity with regard to narrow banding techniques and resonance width, the ratio of the double resonance signal $\Delta V_{\max}$ to the directly observed quadrupole resonance signal V_B of the B spins is found to be

$$\frac{\Delta V_{\max}}{V_B}=\frac{1}{e}\frac{M_{0A}\omega_A\langle\delta_{AB}^2\rangle_{\text{Av}}}{M_{0B}\omega_B\langle\delta_A^2\rangle_{\text{Av}}}. \quad (28)$$

Consider the case of K^{41} in $KClO_3$ having $\langle\delta_A^2\rangle_{\text{Av}}=3.40\times10^5$ sec^{-2} and $\langle\delta_{AB}^2\rangle_{\text{Av}}=0.28\times10^4$ sec^{-2}. K^{41} is 6.9% abundant,[10a] has a magnetic moment of 0.21 NBM with $I=\frac{3}{2}$, and a quadrupole interaction frequency of $\omega_B/2\pi=639.2$ kc at 26°C. For $\omega_A/2\pi=28.1$ Mc at room temperature, a ratio $\Delta V_{\max}/V_B\sim10^3$ is obtained. Figure 3 shows that $\Delta V_{\max}$ for K^{41} yields a measured signal-to-noise ratio of the order of 10 to 20. A search for the K^{41} magnetic resonance absorption in a large magnetic field would not give a signal greater than V_B by more than a factor of 10. We can therefore compensate in those cases where the Boltzmann factor and the Larmor frequency combine to be very small by using the pulsed method. The dipole-dipole interaction expressed by $\langle\delta_{AB}^2\rangle_{\text{Av}}$, combined with a sizable moment M_{0A}, makes possible the indirect detection of the B interactions, which would otherwise be extremely difficult or impossible to measure.

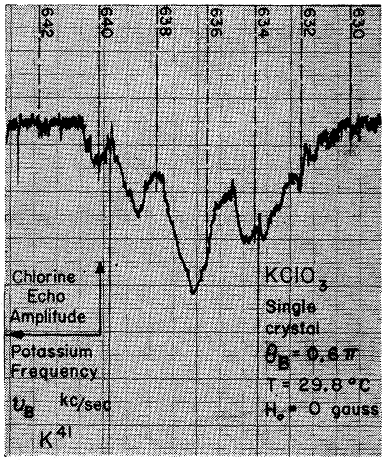

FIG. 3. K^{41} nuclear quadrupole coupling resonance line in $KClO_3$. The structure is due to rf Fourier components in the applied 0.6π radian ($\theta_B=0.6\pi=\gamma_B H_{1B}t_w$) pulse as the K^{41} resonance is traversed in frequency. The resonance frequency has a negative temperature coefficient of ~1 kc/°C.

---

[11] E. M. Purcell, Nuovo cimento **6**, 961 (1957).

[10a] Among extremely dilute spins, with concentrations of 1% or less, C. Kittel and M. Abrahams [Phys. Rev. **90**, 238 (1953)] have shown that the dipolar line broadening is Lorentzian in character. For concentrations of the order of 10% or above, the dipolar broadening is of the approximate Gaussian type which we have assumed. In the limit of extreme dilution, $\Delta V_{\max}$ [Eq. (27)] would then be proportional to

$$(\langle\delta_{AB}^2\rangle_{\text{av}}/\langle\delta_A^2\rangle_{\text{av}})^{\frac{1}{2}}.$$

V. PURE QUADRUPOLE RESONANCE

Excitation of pure quadrupole coupled B nuclei with spin $I>\frac{1}{2}$ produces special effects upon the A-spin echo. Consider the case $I_B=\frac{3}{2}$, where q is an axial electric field gradient, and Q is the nuclear quadrupole moment. In the presence of a magnetic field H_0 such that $\gamma\hbar I_B H_0 \ll eqQ$, two energy levels occur for each value of $m>\frac{1}{2}$:

$$E_{\pm m}=A[3m^2-I(I+1)]\mp m\hbar\gamma H_0\cos\theta, \qquad (29)$$

where $A=e^2qQ/4I(2I+1)$ and θ is the angle between the direction of H_0 and the axis of quantization. These energies correspond to pure states ψ_{+m} and ψ_{-m} respectively. In general, mixed states are obtained in place of pure $m=\pm\frac{1}{2}$ states, given by[8]

$$\psi_\pm=\psi_{\pm\frac{1}{2}}\sin\eta\pm\psi_{\mp\frac{1}{2}}\cos\eta, \qquad (30)$$

having energy eigenvalues,

$$E_\pm=A[\tfrac{3}{4}-I(I+1)]\mp(f/2)\gamma\hbar H_0\cos\theta, \qquad (31)$$

where

$$f=[1+(I+\tfrac{1}{2})^2\tan^2\theta]^{\frac{1}{2}},$$

and

$$\tan\eta=[(f+1)/(f-1)]^{\frac{1}{2}}.$$

A 180° pulse applied at the B-spin resonance frequency $\omega(m\leftrightarrow m+1)=(3A/\hbar)(2|m|+1)$ can pick out, at most, $I-\frac{1}{2}$ resonance transitions. These transitions are dipolar field broadened by an amount of ΔH due to neighbors, and may be strain broadened in addition because of a distribution in q. An externally applied field H_0 will produce discrete Zeeman splitting, particularly for single crystals, but there is evidence of discrete lines, to be shown later, in the case of powdered samples because of the preferential excitation of the rf field H_{1B} upon crystallites oriented in a specific direction with respect to H_0. If the 180° pulse width t_w is sufficiently short[2] so that $\sqrt{3}\gamma_B H_1 t_w=\pi$ (for $I=\frac{3}{2}$) and $1/t_w \gg \gamma_B H_0$, $\gamma_B\Delta H$, then the double resonance of the A spins, seen in terms of $\Delta V(\nu_B)=1-V_d(2\tau)$, measures a broad line having a width $\sim 1/t_w$. The chlorine echo in the absence of double resonance is normalized to unity. In single crystals, where the intensity and direction of H_{1B} can be made the same for all B nuclei in certain salts, such as K in $KClO_3$, Fourier components of the pulse appear in the function $\Delta V(\nu_B)$, as the frequency ν_B of the pulse changes slowly through the line. This structure will be discussed further in the next section.

Assume that the axes of quantization of the A and B spins are the same, which is the case for K and Rb chlorate and nearly so for Cs chlorate. A 180° pulse that excites the $\omega(m\leftrightarrow m+1)$ transition for $m>\frac{1}{2}$ causes the z component of local field at the A nucleus to change by

$$\Delta H_z=\pm\gamma_B\hbar I_B(1-3\cos^2\theta_{AB})/r_{AB}{}^3. \qquad (32)$$

When the pulse excites transitions between states $\psi_{\pm\frac{3}{2}}$ and the mixed states $\psi_\pm$, a more complicated change in local field occurs. Assume that a sufficiently large external field H_0 is applied so that a given pair of A–B spins are decoupled insofar as transitions $\psi_+\leftrightarrow\psi_-$ are concerned. The orientation of a B nucleus in either of the mixed states $\psi_\pm$ is such that $m=+\frac{1}{2}$ and $m=-\frac{1}{2}$ are no longer good quantum numbers which describe constant projections of angular momentum along the quadrupole z axis of quantization. The unitary transformation $T=e^{iI}y^{\cos 2\eta}$, which carries out a rotation of angle 2η about the y axis, defines a new z' axis of quantization at an angle 2η with respect to the quadrupole axis of quantization. Along z' the spin appears to be quantized in pure states $T\psi_\pm$. This proves to be the case, since

$$\langle\psi_\pm T^{-1}|I_z|T\psi_\pm\rangle=\pm\tfrac{1}{2}. \qquad (33)$$

The effective change in local field at the A nuclei is therefore larger for the lowest quadrupole transition frequency $\omega=6A/\hbar$ involving the $\psi_\pm$ states. This transition causes the double resonance signal $\Delta V(2\tau)$ to be stronger than the effect due to all other transitions. For example, when $\theta=\pi/2$, then $\eta=\pi/4$, and the change in local field becomes $\frac{3}{2}\Delta H_z$ instead of ΔH_z given by (32). In addition, another constant component of field appears in the x direction, given by $\Delta H_x=\frac{1}{2}\Delta H_z$. If H_0 is sufficiently small so that the A and B quadrupole systems can couple near zero frequency when they occur in $\psi_\pm$ states, the simple picture above then breaks down. In performing the actual experiment, it is helpful to apply a value of H_0 sufficient to reduce this coupling so that discrete changes in ΔH_z and ΔH_x aid in producing an observable double resonance effect.

The detection of frequencies $\omega(m\leftrightarrow m+1)$ for $m>\frac{1}{2}$ prove also to be more difficult to detect than the lowest frequency, as m increases, because quadrupole strains broaden the line to be observed by an amount proportional to m^2.

VI. EXPERIMENTAL RESULTS

A block diagram of the apparatus is shown in Fig. 4. The instrumentation is essentially the same as that used in early double resonance experiments,[3] except that the B coil is now excited by pulses, and a signal-inte-

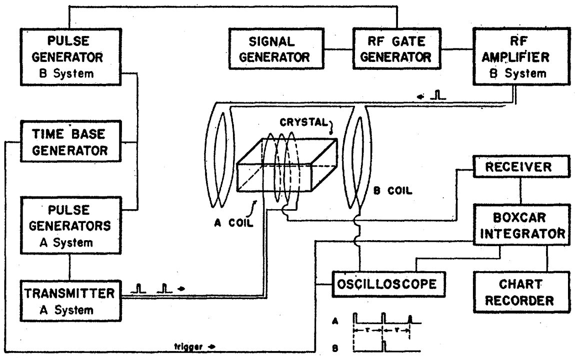

FIG. 4. Double quadrupole resonance apparatus.

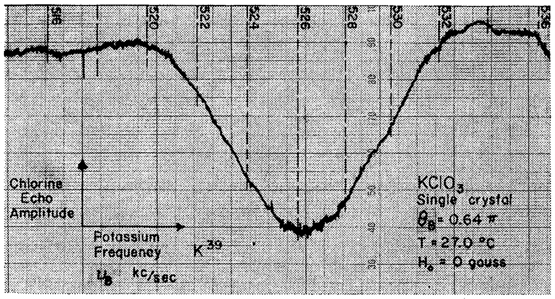

FIG. 5. K^{39} quadrupole double resonance spectrum in KClO$_3$ for $\theta_B=0.64\pi$.

grating "box-car" recorder[12] is used for obtaining greater sensitivity.

The high sensitivity of the double resonance spectroscopy method for detection of B spin resonance is illustrated very well in the case of the K^{41} quadrupole resonance in KClO$_3$, as pointed out in Sec. IV. A further demonstration of the intrinsic high sensitivity may be seen in the excellent signal-to-noise ratio of the K^{39} resonance curves shown in Figs. 5, 6, 7, and 8. The K^{39} pure quadrupole resonance signal would be marginal, at best, in a cw spectrometer with a narrow banded detector. The resonance frequency for K^{39} (KClO$_3$) is 526.5±0.5 kc/sec at 26°±1°C. From the above data, the K^{41}/K^{39} quadrupole moment ratio is 1.22, in close agreement with the value 1.225 obtained from molecular beam techniques.[13]

These figures also illustrate the effect of different pulse widths t_w on the appearance of the double resonance line shape, $\Delta V=1-V_d(2\tau)$, as ω_B passes through the quadrupole resonance having its center frequency at $\omega=\omega(\frac{1}{2}\leftrightarrow\frac{3}{2})$. Let the externally applied field $H_0=0$, and apply an rf field $H_{1B}\gg\Delta H_B$, where ΔH_B is the line width of the B nuclei expressed in gauss. Also the condition $1/t_w\gg\gamma_B\Delta H_B$ applies. The fraction of B neighbors excited by the rf field H_{1B} is given roughly by

$$\beta=(\sqrt{3}\gamma_B{}^2/\epsilon^2)\sin^2(\epsilon t_w/2), \qquad (34)$$

where $\epsilon=[3\gamma_B{}^2H_{1B}{}^2+(\omega_B-\omega)^2]^{\frac{1}{2}}$. As an approximation, let J_j represent the local field due to the jth B spin, and apply the formula given by Eq. (4). $V_d(2\tau)$ may be written as

$$V_d(2\tau)=\prod_j^N[1-2\beta\sin^2(J_j\tau/2)]$$
$$=[1-2\beta\sin^2(J_{\mathrm{Av}}\tau/2)]^N, \qquad (35)$$

if we let J_{Av} be an average local field and note that $\alpha+\beta=1$. The signal, $\Delta V=1-V_d(2\tau)$, which varies through maxima and minima, is symmetric about the resonance at $\omega_B-\omega=0$. The maxima occur when $(\omega_B-\omega)_n=\pm(2\pi/t_w)[n(n+1)]^{\frac{1}{2}}$. The integer $n=1$, 2, 3, $\cdots$ pertains to successive satellite maxima in the order of decreasing amplitude of ΔV. Figures 6 and 7 show a rough agreement with this prediction. The maxima do not occur exactly as predicted but are shifted slightly toward the center because of the effect of attenuation off resonance. The pulse width t_w, applied to give the signal in Fig. 7, is adjusted to be about twice the value used to obtain the plot in Fig. 6. Figure 5 shows the broadening effect of a much shorter pulse.

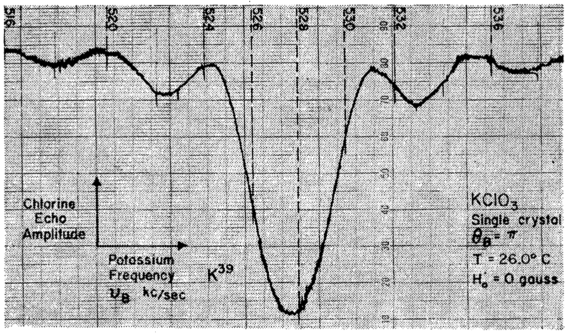

FIG. 6. K^{39} quadrupole double resonance spectrum in KClO$_3$ for $\theta_B=\pi$.

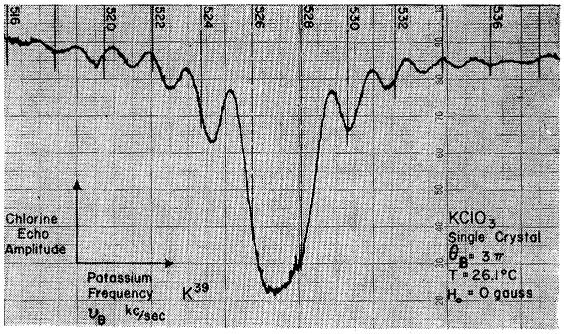

FIG. 7. K^{39} quadrupole double resonance spectrum in KClO$_3$ for $\theta_B=3\pi$.

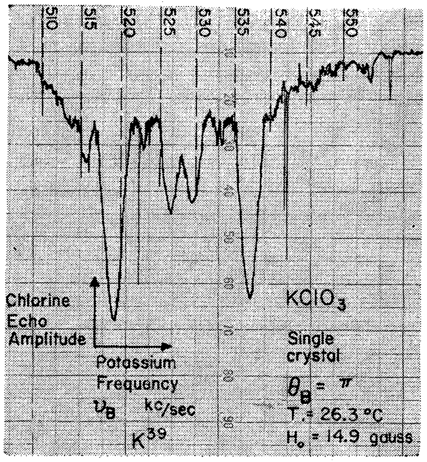

FIG. 8. K^{39} quadrupole double resonance spectrum in KClO$_3$ with Zeeman splitting present.

---

[12] D. Holcomb and R. E. Norberg, Phys. Rev. 98, 1074 (1955).

[13] C. A. Lee, B. P. Fabricand, R. O. Carlson, and I. I. Rabi, Phys. Rev. 91, 1395 (1954).

If a very wide pulse is used with the intent of eliminating the above Fourier components, it is again difficult to obtain a true measure of B-resonance line shape, because H_{1B} becomes comparable to or less than ΔH_B, and $1/t_w \lesssim \gamma \Delta H_B$. A unique 180° pulse at resonance therefore cannot be defined, making the analysis of ΔV extremely complex. The amplitude of ΔV is then described better by the steady-state double resonance analysis,[3] in which case ΔV provides a more reliable measurement of the B-resonance line shape. The double resonance of powdered samples is, of course, much more difficult to analyze because of a distribution in rf fields for both the A and B resonances. Externally applied magnetic fields H_0 further complicate the situation. The pulsed double resonance method is obviously not convenient for line shape measurements.

If a small magnetic field H_0 is applied to the single crystal, a Zeeman splitting of the degenerate quadrupole energy levels will be produced.[2] The specific form of the splitting is, in general, a function of the relative orientation of the crystalline axis of quantization and the magnetic field direction. For a system with spin $I=\frac{3}{2}$, four lines at most can appear, such as in Fig. 8, which shows the double-resonance spectroscopy of K^{39} in a magnetic field of $H_0=14.9$ gauss.

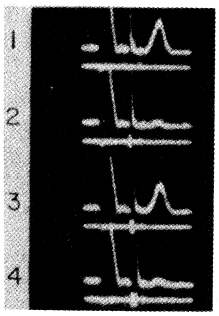

FIG. 9. Effect of K^{39} double resonance upon the Cl^{35} echo amplitude in $KClO_3$. Frames 1, 2, 3, and 4 show respectively the B pulse width (below each chlorine echo trace) for θ values of 0°, 180°, 360°, and 540°.

Equation (35) predicts a sinusoidal dependence of the A echo amplitude upon the B pulse width t_w, when $\omega=\omega_B$, making $\beta=\sin^2(\sqrt{3}\gamma_B H_{1B} t_w/2)=\sin^2(\theta/2)$. In Fig. 9, the frames 1, 2, 3, 4 show the effects when t_w is adjusted to give θ values of 0°, 180°, 360°, 540° respectively in monocrystalline $KClO_3$. In polycrystalline $KClO_3$, the variation in echo amplitude, although less pronounced because of the random orientation of spin quantization axes, is still easily observable.

From the simple model expressed by Eq. (3), it is to be expected that the perturbing effect on the A spin echo of B spin double resonance depends upon the application time t' of the B pulse with respect to the pulse sequence creating the A spin echo, assuming an average over many J values. In particular, for fixed B pulse width, a maximum A echo degradation is expected when the B pulse application time $t'=\tau$. No effect should occur if $t'=0$ or 2τ. When the A echo amplitude for $NaBrO_3$ and $KClO_3$ is measured, with the application time t' of a B-system 180° pulse varied between 0 and τ, the predicted echo amplitude dependence upon $\exp(-t'^2/T_{AB}^2)$ is found to be closely followed, where $1/T_{AB}^2 \approx J_{\text{Av}}^2/2$ and $J_{\text{Av}}^2 \approx 4\langle \delta_{AB}^2 \rangle_{\text{Av}}$.

TABLE I. Cl^{35} nuclear quadrupole resonance in chlorates at 24°C.[a]

Substance	Frequency Mc/sec	T_1 millisec
$NaClO_3$	29.90	45
$KClO_3$	28.08	21
$RbClO_3$	28.81	29
$CsClO_3$	28.37	52

[a] The T_1 measurements are accurate to ±2 milliseconds.

VII. QUADRUPOLE RESONANCES

Chlorine

The nuclear quadrupole resonance frequencies of Cl^{35} in the alkali chlorates have been reported in the literature,[8,14] except for $LiClO_3$. We have made an unsuccessful search for the chlorine resonance in this compound. The strong deliquescent nature of $LiClO_3$ apparently prevents the formation of a definite crystal structure.

The Cl^{35} spin-lattice relaxation times (T_1) were measured by the growth of the free-precession tail following the second of two 90° pulses. With the rubidium and cesium chlorates, it was necessary to measure the growth of an echo, since the free-precession tails were masked by piezoelectric vibrations. The pulse program consisted of a closely-spaced 90°–180° sequence, followed at a variable delay by a similar 90°–180° sequence. The first two pulses saturate the sample, and the second pair forms an echo with an amplitude proportional to the spin-lattice relaxation that takes place between the two sequences. Both methods above were compared in the measurement of the chlorine relaxation in sodium chlorate, and the measurements agree within experimental error (see Table I).

Rubidium

The $RbClO_3$ and $CsClO_3$ compounds were studied in powder form, since it was difficult to obtain single crystals of these compounds. The alkali resonance line widths in $NaClO_3$ and $KClO_3$ appear to be intrinsically narrow, since the double resonance line shapes were determined primarily by the B pulse spectrum. In rubidium chlorate, the indicated lines were quite broad, shown by the fact that only the most intense narrow pulses could increase the apparent line width (Fig. 10).

Although a powdered sample is studied, the presence of a magnetic field can give rise, surprisingly, to a Zeeman pattern in the double resonance experiments. The coil that excites and receives the signal from the Cl^{35} nuclei responds mostly to those nuclei which have

---

[14] M. Emshwiller and E. L. Hahn, Bull. Am. Phys. Soc. 3, 318 (1958).

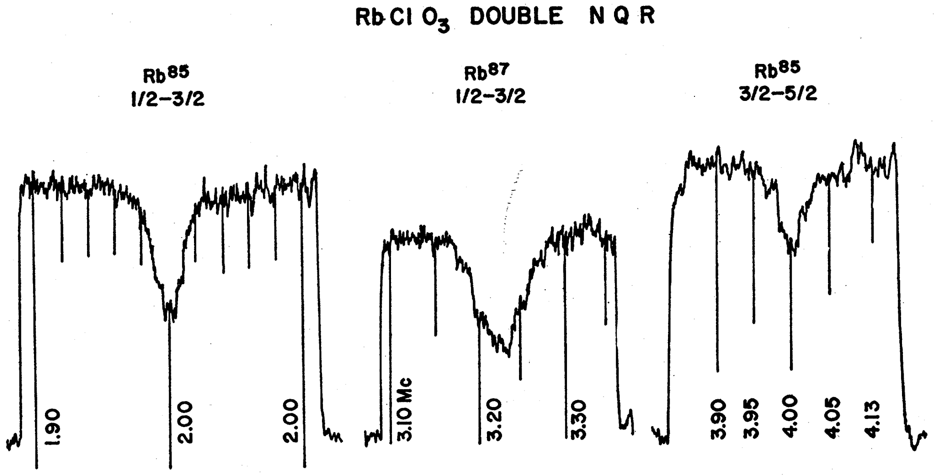

FIG. 10. Quadrupole double resonance spectra of rubidium isotopes in RbClO$_3$.

their axes of quantization perpendicular to the coil. The alkali nuclei also have a similar preferential plane perpendicular to the B coil. In all cases studied, the Cl^{35} and alkali ion axes of quantization are essentially the same. In the experimental apparatus, the two coils are mutually orthogonal, and hence only those crystal orientations which provide axes of quantization perpendicular to the axes of both coils will contribute strongly to the double resonance echo degradation. This selection of a preferred direction, although somewhat diffuse, allows a Zeeman structure to be manifested in the double resonance line. An increase in double resonance sensitivity by roughly 20% to 40% is obtained in powdered samples if the A and B coils are parallel, because most crystallites, with their quantization axes lying in a plane perpendicular to the common axis, participate in the resonance.

In the Rb line, at 2 Mc/sec, there is a clear split of the central line and indications of two satellites or shoulders. These traces were made with a small movable permanent magnet placed near the sample in order to maximize the Cl^{35} echo lifetime. The strength and orientation of this field, not determined with any accuracy, accounts for some of the line width of the observed lines. In particular, this effect would lead to a broader Rb^{87} line than the Rb^{85} lines, since the former nucleus has a larger gyromagnetic ratio.

In the case of spins larger than $\frac{3}{2}$, it is expected that the transitions among higher m values, excluding the transition $\omega(\frac{1}{2}\leftrightarrow\frac{3}{2})$, provides smaller values of ΔV, according to the discussion in Sec. V. This can be seen from an inspection of the signal-to-noise ratio of the resonances shown in Fig. 10.

Cesium

The small quadrupole moment of Cs^{133} ($I=\frac{7}{2}$) gives rise to low quadrupole frequencies, ranging from 9 to 54 kc/sec [see Table II and Fig. 11(a)]. Ratios of 1:2:3 are observed, approximately, for the single stable isotope having $I=\frac{7}{2}$, coupled to a nearly pure axial field gradient.

Upon increasing the intensity of the pulse field H_{1B}, additional lines appear [Fig. 11(b)] in the absence of a

TABLE II. Alkali chlorates, alkali resonance.

Alkali nucleus	Abundance	Spin	Quadrupole[a] moment $\times10^{24}$ cm^2	Transitions	Frequency[b]
Na^{23}	1.00	$\frac{3}{2}$	$\sim$0.1	$\frac{1}{2}:\frac{3}{2}$	396.0 kc/sec ±0.5 kc/sec
K^{39}	0.93	$\frac{3}{2}$	0.07	$\frac{1}{2}:\frac{3}{2}$	526.5 kc/sec ±0.5 kc/sec
K^{41}	0.07	$\frac{3}{2}$	0.085	$\frac{1}{2}:\frac{3}{2}$	639.2 kc/sec ±0.5 kc/sec
Rb^{85}	0.73	$\frac{5}{2}$	0.31	$\frac{1}{2}:\frac{3}{2}$	2.00 Mc/sec±0.01 Mc/sec
				$\frac{3}{2}:\frac{5}{2}$	4.00 Mc/sec±0.01 Mc/sec
Rb^{87}	0.27	$\frac{3}{2}$	0.15	$\frac{1}{2}:\frac{3}{2}$	3.22 Mc/sec±0.01 Mc/sec
Cs^{133}	1.00	$\frac{7}{2}$	0.003	$\frac{1}{2}:\frac{3}{2}$	18.2 kc/sec ±0.3 kc/sec
				$\frac{3}{2}:\frac{5}{2}$	35.2 kc/sec ±0.3 kc/sec
				$\frac{5}{2}:\frac{7}{2}$	53.0 kc/sec ±0.3 kc/sec
				$\Delta m=2$	
				$\mp\frac{1}{2}:\pm\frac{3}{2}$	9.0 kc/sec ±0.3 kc/sec
				$\pm\frac{1}{2}:\pm\frac{5}{2}$	27.3 kc/sec ±0.3 kc/sec
				$\pm\frac{3}{2}:\pm\frac{7}{2}$	44.0 kc/sec ±0.3 kc/sec

[a] W. A. Nierenberg, *Annual Review of Nuclear Science* (Annual Reviews, Inc., Palo Alto, 1957), Vol. 7, p. 349.
[b] Data taken at temperature $T=26°\pm1°$C.

field H_0, which are attributed to double quantum transitions[15] occurring at frequencies

$$\omega_d = (1/2\hbar)(E_m - E_{m-2}),$$

for $m=\frac{7}{2}$ and $\frac{5}{2}$, corresponding to frequencies 44.0 kc/sec and 27.3 kc/sec. A third transition at 9.0 kc/sec occurs between the $m=\pm\frac{3}{2}$ levels and the lower levels which are in mixed states. Double quantum transitions become highly probable, since the rf field energy $\gamma\hbar I_B H_{1B}$ can be made comparable to the low quadrupole coupling energy eqQ. The change in Cs dipolar field at Cl sites is increased by a factor of two for these transitions, and indeed the echo signal degradation ΔV is actually larger than, or at least equivalent to, the ΔV due to the single quantum transitions. As seen from Fig. 11(b), the double quantum transition at 44 kc/sec causes a greater change in echo amplitude than the single quantum transitions at 36 and 54 kc/sec. The 18 kc/sec single quantum transition produces a large effect due to the presence of mixed states, as pointed out in Sec. V.

At low pulse power, double resonance transitions also track the presence of a small Zeeman splitting when a small field H_0 is applied, in this case, perpendicular to the plane defined by the A and B coil axes as seen in Fig. 11(c). The double resonance is particularly effective for those crystallites having H_0 parallel to the axis of quantization, since H_{1B} is perpendicular to H_0. Figure 11(d) now indicates how double quantum transitions sense the Zeeman splitting as well, with increased pulsed power.

Close examination of these frequencies of low pulse fields H_{1B} reveals that the resonant frequencies of Cs in cesium chlorate are not in the ratio 1:2:3. This implies a finite value for the asymmetry field gradient parameter η, in terms of second derivatives of the potential V, defined as

$$\eta = (V_{XX} - V_{YY})/V_{ZZ},$$

if

$$|V_{ZZ}| \geqq |V_{YY}| \geqq |V_{XX}|.$$

The energy levels as a function of η have been calculated by Cohen[16] for one-tenth-integer values of η. The measured frequencies are 18.2, 35.2, and 53.0 kc/sec, accurate to ±0.3 kc/sec. These frequencies are in the ratios of 2.06, 3.98, and 5.99, with an accuracy of $\sim 1\%$, which compares with the data of Cohen best at a value of $\eta=0.1$ for theoretical ratios 2.071:3.978:5.994. The estimate of the asymmetry at the cesium sites is, therefore, $\eta = 0.1 \pm 0.02$.

VIII. CONCLUSIONS

General features of the spectra produced by pulsed nuclear double resonance have been described. The shape and magnitude of the B spin signal depend upon the rf pulse field intensity applied to the B spins, the rf pulse width, the amount of dipole-dipole coupling between A and B spins, and the spin-spin relaxation caused by the dipole-dipole coupling. The signal strengths obtained by the pulsed method can exceed, by orders of magnitude, those signal strengths obtained by direct observation of the conventional nuclear resonance.

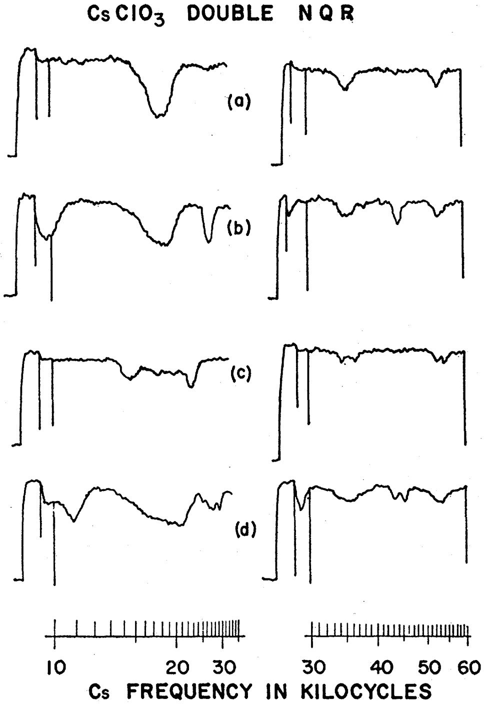

FIG. 11. Quadrupole double resonance spectra of Cs^{133} transitions in $CsClO_3$. (a) Low B pulse power and magnetic field $H_0=0$. (b) High B pulse power and magnetic field $H_0=0$. (c) Low B pulse power and magnetic field $H_0\neq 0$. (d) High B pulse power and magnetic field $H_0\neq 0$.

We have featured a novel technique in this paper, and are not interested in presenting arguments here which account for the nuclear quadrupole interactions in alkali chlorates measured by our method. Bersohn[17] has discussed a method of machine computation for components of the electric field gradient at the sites of alkali nuclei in alkali chlorates. Upon incorporation of the appropriate Sternheimer electric shielding factor[18] with these computations, Bersohn obtains values of e^2qQ for Na in $NaNO_3$ and $NaClO_3$. These theoretical values are in rough agreement with measured values, if Q values are taken from the results of molecular beam measurements. We have applied Bersohn's calculation to the case of K^{39} and K^{41} in $KClO_3$ and find such an agreement also, but have not extended it to other cases measured by us. Aside from studies of the alkali metals, it should be possible to amass data for

---

[15] V. Hughes and L. Grabner, Phys. Rev. **79**, 314 (1950); P. P. Sorokin, I. L. Gelles, and W. V. Smith, Phys. Rev. **112**, 1513 (1958).

[16] M. H. Cohen, Phys. Rev. **96**, 1278 (1954).

[17] R. Bersohn, J. Chem. Phys. **29**, 326 (1958).

[18] T. P. Das and R. Bersohn, Phys. Rev. **102**, 733 (1956); E. G. Wikner and T. P. Das, Phys. Rev. **109**, 360 (1958).

the little studied interactions of nuclei such as D^2 and N^{14} in crystals. Application of a magnetic field, of course, permits the measurement of gyromagnetic ratios of nuclear moments as well.

A clear interpretation of resonance line shapes and splittings in solids does not appear to be available from pulsed double resonance spectra, although the symmetry displayed enables the resonance frequency to be accurately determined. Line shape analysis is difficult because of complicated effects due to Fourier frequency components in the B spin pulse, and because a rigorous quantum mechanical analysis of echo signals in solids does not exist. In spite of these weaknesses, a stochastic Gaussian model for spin-spin interactions accounts, at least qualitatively, for the observed signal shapes, and allows for a rough determination of the component mean square local field due to B spins which are coupled to the A spins. In cases where the A and B spins are coupled in relatively isolated pairs, it would be possible to measure the direction and rough magnitude of the dipole-dipole coupling by measurement of the double resonance signal amplitude ΔV as a function of orientation angle θ_{AB}.

In liquids the indirect spin-spin interaction constant J can be measured in general between different nuclei by the pulsed double resonance method. However, identical information can also be obtained by application of conventional nuclear magnetic resonance spectroscopy.

ACKNOWLEDGMENTS

We wish to thank Dr. T. P. Das and Professor R. Bersohn for informative discussions.

APPENDIX A

Let $c(t)$ be a correlation function which expresses the remnant precessional coherence of an ensemble of spins after a time t. Assume that

$$S_A(t)=\exp\left[i\int_0^t \delta(t')dt'\right]=\exp(i\delta_0 t)c(t)+Z(t) \quad \text{(A.1)}$$

is the precession vector of a packet of A spins having a Larmor frequency δ_0 in the moving frame at $t=0$, and $Z(t)$ is a complex vector having a random distribution of phases at time t. At $t=0$, $c(t)=1$ and $Z(0)=0$. Also $\langle Z(t)\rangle_{\text{Av}}=0$, $\langle\exp(i\delta_0 t)\rangle=\langle U(t)\rangle=T_0(t)$, $\langle Z(t)\exp(i\delta_0 t)\rangle=0$, and $\langle Z(t)Z(t')\rangle\neq0$, where t' can be different from, or the same as, t. First the A–A spin interaction is neglected by dropping the C_{jk} and D_{jk} terms in Eq. (9). The expression $\langle U(t)\rangle$ is a measure of the free-induction signal computed from (9), excluding the terms $C_{j'k'}$, while the expression $\langle T(t)\rangle=\langle S(t)\rangle=\langle\exp(i\delta_0 t)c(t)\rangle$ gives the free-induction signal which includes the effect of these terms. Let the nth moment of the resonance line be given by $\langle\Delta\omega_0{}^n\rangle$ when $C_{j'k'}$ is excluded, and by $\langle\Delta\omega^n\rangle$ when it is included. Then

$$T_0(t)=\sum_{n=0}^{\infty}\frac{i^{2n}\langle\Delta\omega_0{}^n\rangle t^n}{n!},$$

and

$$T(t)=\sum_{n=0}^{\infty}\frac{i^{2n}\langle\Delta\omega^n\rangle t^n}{n!}.$$

The 90°–180° free-precession function is given by

$$\begin{aligned}S_{A,B,B'}&=\exp\left[-i\int_0^\tau \delta(t')dt'+i\int_\tau^{\tau+t}\delta(t')dt'\right]\\&=\exp\left[-2i\int_0^\tau \delta(t')dt'+i\int_0^{\tau+t}\delta(t')dt'\right]\\&=\{\exp(-i\delta_0\tau)c(\tau)+Z^*(\tau)\}^2\\&\quad\times\{\exp[i\delta_0(\tau+t)]c(\tau+t)+Z(\tau+t)\}, \quad \text{(A.2)}\end{aligned}$$

using (A.1). Upon multiplying out (A.2) and carefully evaluating average values of the cross terms, the average echo amplitude at time t is given by

$$\langle S_{A,B,B'}(t)\rangle=E_{A,B,B'}(t)=\frac{2T_0(t-2\tau)T(\tau)^2T(t)}{T_0(\tau)^2[T_0(t)+T(t)]}. \quad \text{(A.3)}$$

The echo maximum occurs roughly at $t=2\tau$ and $T_0(0)=1$. Equation (A.3) accounts for the interaction of A spins with B and B' spins. Inclusion of the A–A spin interaction is approximated by writing

$$E_{A,A,B,B'}(t)=E_{A,B,B'}(t)T_{AA}(t), \quad \text{(A.4)}$$

where $T_{AA}(t)$ now includes the C_{jk} and D_{jk} terms. If a 180° double resonance pulse is applied to the B spins at $t=\tau$, the expression $E_{A,B'}(t)$ replaces $E_{A,B,B'}(t)$ in (A.4), meaning that the B spins are excluded from influencing the virtual echo term $E_{A,B'}(t)$, and is considered instead in an added factor $T_{AB}(t)$. The reduced amplitude then becomes

$$E_{A,A,B,B'}(t)_{\text{doub. res.}}=E_{A,B'}(t)T_{AA}(t)T_{AB}(t). \quad \text{(A.5)}$$

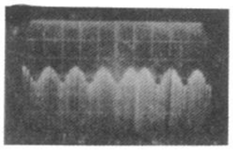

FIG. 1. Modulation of proton echo envelope due to double resonance of P nuclei in $HPO(OH)_2$ as a function of time t' [see Eq. (3)]. The oscillogram pattern extends over a total time of 10 milliseconds. The phase shift occurs at a time $\tau=6.2$ milliseconds. Zero echo amplitude baseline is below the oscilloscope face.

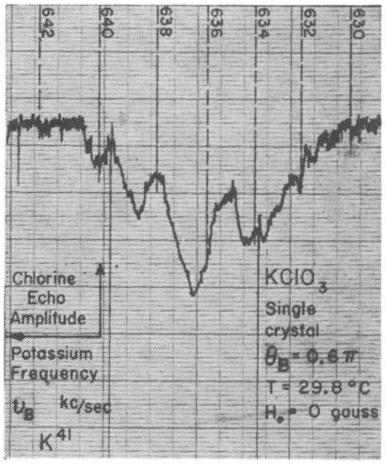

FIG. 3. K^{41} nuclear quadrupole coupling resonance line in $KClO_3$. The structure is due to rf Fourier components in the applied 0.6π radian ($\theta_B=0.6\pi=\gamma_B H_{1B} t_w$) pulse as the K^{41} resonance is traversed in frequency. The resonance frequency has a negative temperature coefficient of $\sim$1 kc/°C.

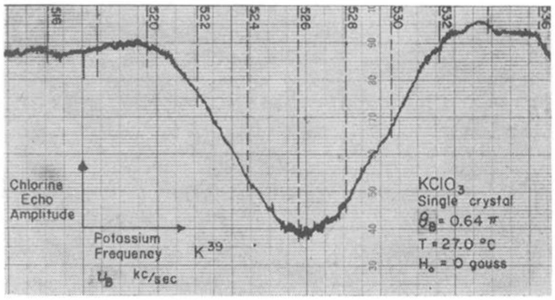

FIG. 5. K^{39} quadrupole double resonance spectrum in $KClO_3$ for $\theta_B=0.64\pi$.

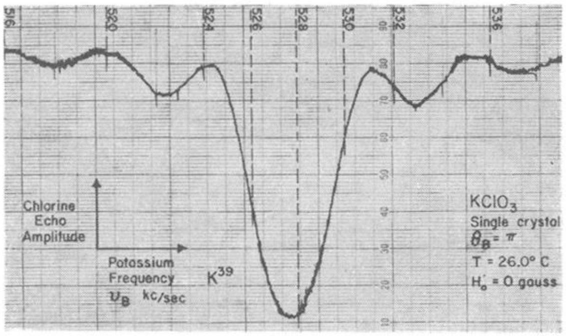

FIG. 6. K^{39} quadrupole double resonance spectrum in $KClO_3$ for $\theta_B=\pi$.

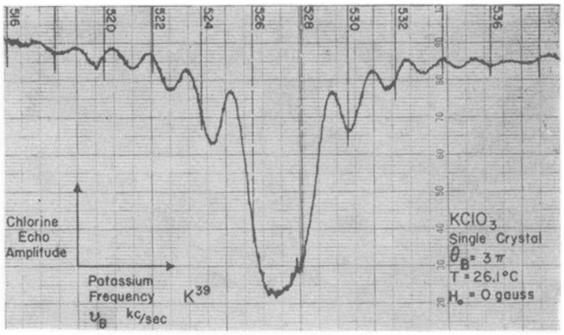

FIG. 7. K^{39} quadrupole double resonance spectrum in $KClO_3$ for $\theta_B = 3\pi$.

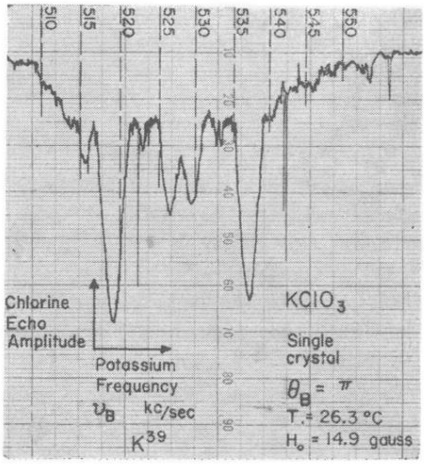

FIG. 8. K^{39} quadrupole double resonance spectrum in $KClO_3$ with Zeeman splitting present.

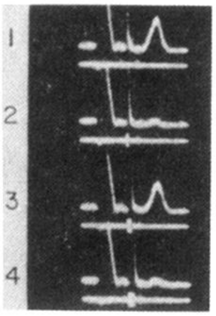

FIG. 9. Effect of K^{39} double resonance upon the Cl^{35} echo amplitude in $KClO_3$. Frames 1, 2, 3, and 4 show respectively the B pulse width (below each chlorine echo trace) for θ values of 0°, 180°, 360°, and 540°.